New Horizons in Earth Reinforcement – Otani, Miyata & Mukunoki (eds)

Effect of facing rigidity on the stability of nailed sand slope in model tests

N. Mikami & K. Okazaki
Nittoc Construction Co., LTD., Japan

D. Hirakawa & F. Tatsuoka
Department of Civil Engineering, Tokyo University of Science, Japan

C.C. Huang
Department of Civil Engineering, National Cheng Kung University, Taiwan

ABSTRACT: A series of loading tests on nailed model sand slope covered with various types of facing was performed to investigate the effect of facing rigidity on the load-settlement behavior of nailed slopes loaded on its crest. The test results showed that the ultimate bearing capacity (i.e., the stability) of the nailed slope was effectively increased with an increase in the facing rigidity by using continuous stiff and/or flexible panel facings. It was also shown that the post-yielding strain hardening behavior of the nailed slope becomes significantly ductile by using effectively facing having a relevant rigidity.

1 INTRODUCTION

Facings are conventionally used as one of the essential structural components for reinforced or nailed slopes. However, the contribution of facings to the stability of reinforced slopes is rather poorly understood and is yet to be addressed in the current design guidelines. Gutierrez and Tatsuoka (1988) pioneered an experimental study focusing on the mechanical contribution of facing to the stability of reinforced slopes by performing loading tests on a footing placed on the crest of reinforced sandy slope. They found that the bearing capacity of reinforced slope increases by using a rigid facing of which connected to the nails. However, reports of similar experiments using facings having different degrees of rigidity cannot be found in the literature.

The present study investigated the effects of facing rigidity on the stability of nailed slope by performing loading tests on a footing placed on the crest of nailed model sandy slopes with a wide variety of facing rigidities. Numerical stability analysis on these tests is reported in the companion paper (Huang et al., 2007).

2 LOADING TESTS ON MODEL SLOPES

Figure 1 shows the test set-up in the present study. The model sandy slope was constructed using

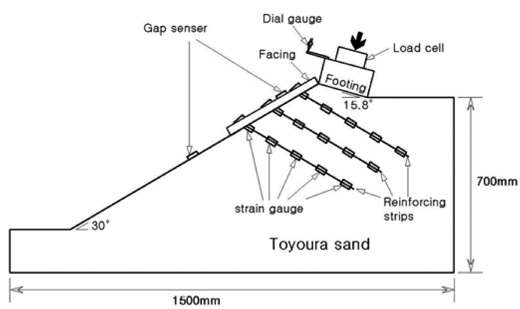

Figure 1. Configuration and geometry of loading test.

Toyoura sand, which is a uniform subangular fine sand ($e_{\max} = 0.933$, $e_{\min} = 0.624$, $G_s = 2.650$, $D_{50} = 0.179$ mm). The model was prepared by pluviating air-dried particles of Toyoura sand through air using multiple sieves. Table 1 shows the average dry unit weight (γ_{d}) of the model slopes. The surface of a sand mound was trimmed to form a slope with an angle of inclination from the horizontal, $\alpha = 30°$, and the top of slope was trimmed to form an inclined loading plane (15.8° inclined-backward) for placing a 100 mm-wide rigid footing as shown in Fig. 1.

Four types of facing having largely different rigidity (or strength) were prepared by using different natural or artificial materials listed in Table 2. Phosphor bronze strips, 3 mm-wide, 0.5 mm-thick and

Table 1. Summary of test conditions and results.

Test name	Reinforcement	Facing type	Φ_t	Φ_p	Dry density (kN/m^3)	q at 5 mm (kN/m^2)	q at 10 mm (kN/m^2)	q at 20 mm (kN/m^2)	Yielding point (kN/m^2)
1	Yes	Agar + cotton yarns	39.6	44.2	14.75	54.9	53.6	77.3	57.5 at 5.65 mm
2	Yes	Bearing plate (15 mm* 15 mm)	39.3	43.8	14.7	32.7	37.0	47.0	33.8 at 7.34 mm
3	Yes	Cement bentonite + Plyester yarns	39.8	44.4	14.79	58.1	71.0	86.8	70.5 at 9.04 mm
4	Yes	Non-woven filter	39	43.5	14.66	37.5	42.2	56.8	37.2 at 4.51 mm
5	Yes	No	40.9	45.8	14.98	30.9	33.3	42.8	32.7 at 9.29 mm
6	No	No	42.6	47.7	15.28	34.0	31.7	39.6	33.0 at 11.22 mm

Table 2. Facing types and material properties.

Facing type	Materials	Size	Tensile strength (100 mm-wide)
1	Agar + Cotton yarns	0.4 m*0.3 m	25 N
2	Bearing Plate	0.15 m*0.15 m	>300 N
3	Cement bentoine + Polyester yarns	0.4 m*0.3 m	>100 N
4	Non-woven filter	0.4 m*0.3 m	84 N

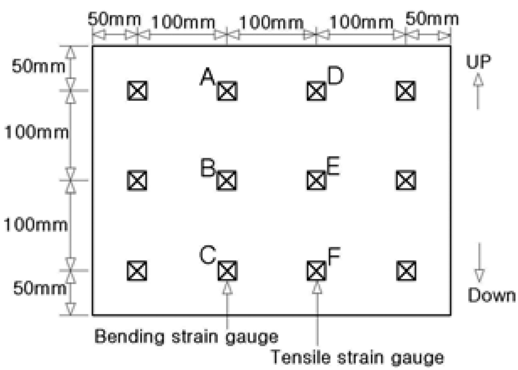

Figure 2. Front view of facing plate and locations of reinforcing bars.

250 mm-long, were used as model tensile reinforcement members simulating prototype soil nails. These strips were placed with a vertical and horizontal center-to-center spacing of 100 mm and the top ends were fixed to the back face of facing in some of the tests. An unreinforced slope without facing (Test No. 6) and a reinforced slope without facing (Test No. 5) were performed as baseline tests. The front view of the facing and the reinforcement configurations are show in Fig. 2. Electric-resistant strain gages were attached to the reinforcing strips at the positions shown in Fig. 3. The surface of strips and strain gages were coated using epoxy and Toyoura sand particles to simulate a rough soil-reinforcement interface condition.

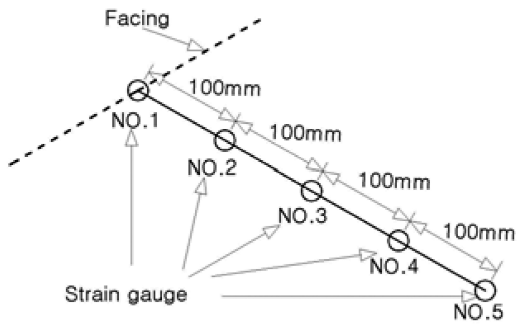

Figure 3. Schematic view of reinforcing strip and locations of strain gauges.

A 100 mm-wide rigid footing was loaded at a constant displacement rate in the direction normal to its base. Five two-component load cells, which measure normal and shear load simultaneously with negligible coupling effects, were mounted on the central third of the base of the 400 mm-long footing to eliminate the influence of the boundary friction from the sidewalls of the sand box. Displacement of the footing was measured using a displacement transducer and the deformation of facing and slope surface were measured using proximity transducers (i.e., gap sensors) as shown in Fig. 1.

3 TEST RESULTS AND DISCUSSIONS

Figure 4 shows the relationships between the total normal footing load (P_F) and the footing settlement (S) in the direction normal to the footing base. As this load was measured using a load cell arranged between the footing and the loading piston, it includes the boundary friction and it is greater by about 10% than the value measured using the load cells mounted at the central third of the footing. The following trends can be seen from Fig. 4:

1) The behaviors of the unreinforced slope and the reinforced slope without facing (Test Nos. 5 and

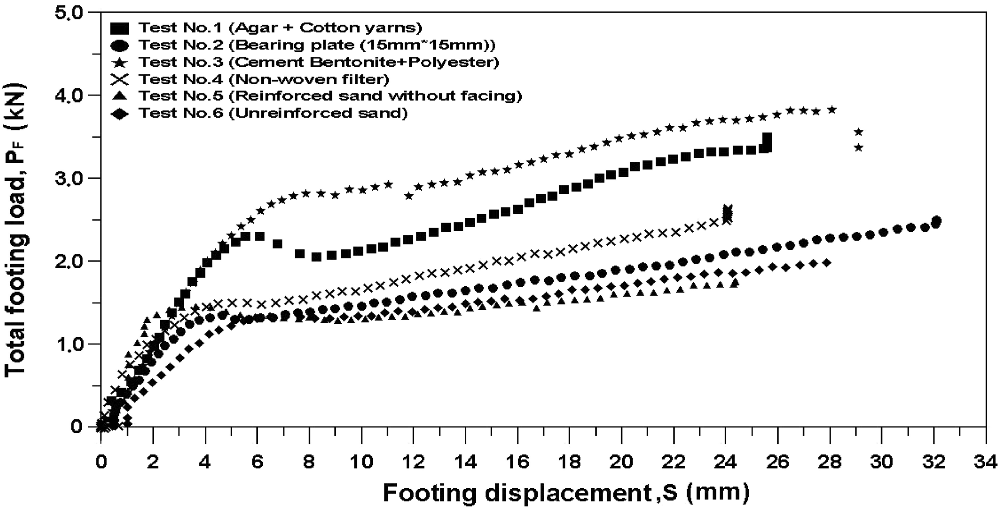

Figure 4. Total footing load (PF) vs. footing displacement (S) relations for reinforced and unreinforced slopes.

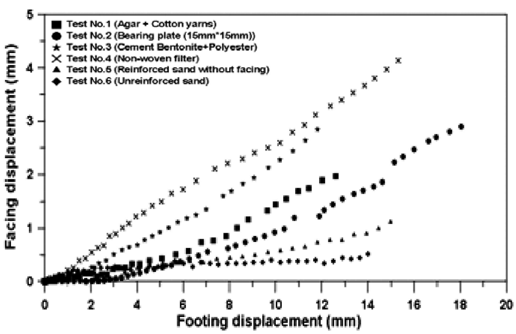

Figure 5a. Normal displacement of facing at 100 mm from the slope crest.

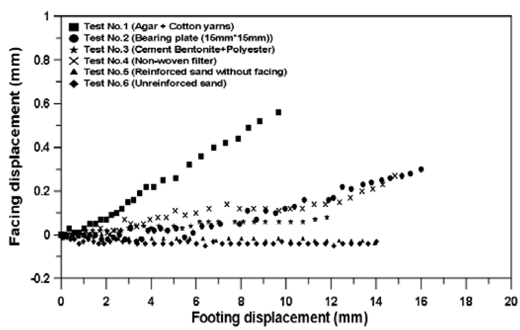

Figure 5b. Normal displacement of slope face at 400 mm from the slope crest.

6) are rather similar. However, when taking into account the fact that the unreinforced sand slope was denser than the reinforced slope without facing and comparing the behaviours for the same sand density, the unreinforced slope should become noticeably weaker than the reinforced slope without facing.

2) Two reinforced slopes with type 1 and type 3 facings (Test Nos. 1 and 3) are much stronger than these two slopes described above. Again, when taking into account that the slopes in Tests Nos. 1–4 are generally looser than those in Tests Nos. 5 & 6 and comparing the behaviours for the same sand density, the effects of facing rigidity should have become larger than those seen from Fig. 4.

Fig. 5(a) shows the heaving of the facing in the direction normal to the slope face measured at a 100 mm distance from the slope crest (see Fig. 1). It can be seen the deformations of the reinforced slopes are generally larger than the unreinforced slope and the reinforced slope without facing. It is like that these two slopes failed under the 'punching' mode due to a low strength of the sand zone below the footing because of no reinforcing (Test No. 6) or small reinforcing effects resulting from free top conditions of reinforcement (Test No. 5). On the other hand, it is like that the failure of the reinforced slope with facing was more general associated with load re-distribution and soil confinement within the more stabilized reinforced zone. Fig. 5(b) shows the heaving of slope surface measured at a 400 mm distance from the slope crest. It can be seen that only the test using type 1 facing (agar + cotton yarns) has a distinctly large deformation compared with the others. This trend may be attributed to the load re-distribution

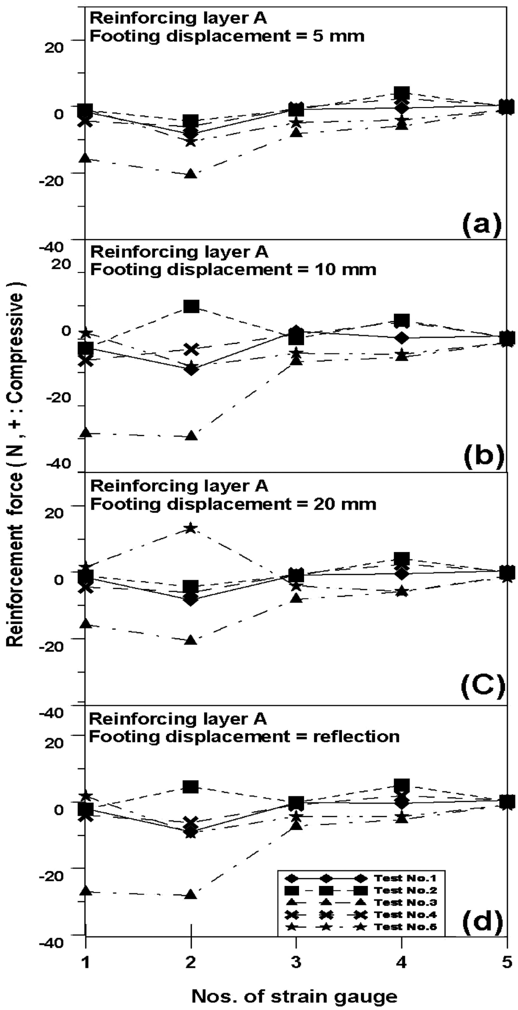

Figure 6. Reinforcement force activated in the top reinforcement layer measured at various footing settlements: a) 5 mm, b) 10 mm and c) 20 mm, and d) at yielding point.

mechanism induced by the 'wide-slab' effect formed in the reinforced zone as reported by Huang and Tatsuoka (1994). This wide-slab mechanism may account for the large value of q (=57.5 kN/m^2 at yield point which is second largest one among the six tests performed).

Figs. 6a)–d) show the tensile force in the uppermost layer of reinforcement 'A' at various strain gage locations (shown in Fig. 1) measured when the footing settlement S was equal to 5 mm, 10 mm and 20 mm and when the load-settlement relation exhibited a yielding point. The tensile force is always highest in Test No. 3 among all the tests regardless of the footing settlements. This is consistent with the largest footing pressure *q* in this test, as summarized in Table 1. It is also important to note that the test results indicate high connection force at the back of the facing, which is essential to activate high reinforcing effects.

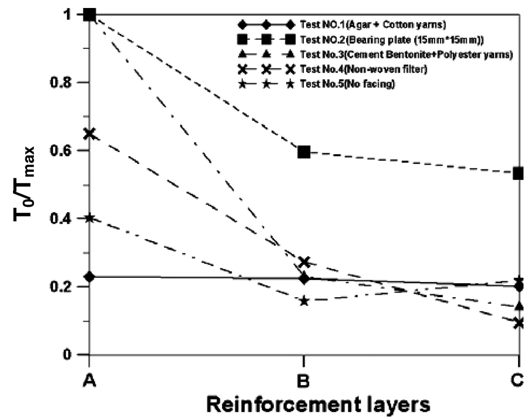

Figure 7. Measured values of T0/Tmax in the top reinforcement layer measured at the yield point.

Fig. 7 compares the values of T_o/T_{max}, where T_o is the reinforcement force developed adjacent to the slope surface, and T_{max} is the maximum tensile force among the three reinforcement layers A, B and C in all the tests, measured at the yielding point of the footing load-settlement (P_F – S) curve. It can be seen that Test Nos. 2 and 3 using facings that had locally or globally highest bending stiffness exhibit highest values of T_o/T_{max}. The values of T_o/T_{max} in the other tests fall between 0.2 and 1.0. The second highest value of *q* measured in Test No. 1 is inconsistent with the fact that the measured reinforced force is relatively low. This trend of behavior may be related to the 'wide-slab' effect and a future study into this point is necessary. Despite that the above, the general trend is an increase in the footing pressure (i.e., an increase in the slope stability) with an increase in the T_o/T_{max} value associated with an increase in the facing rigidity.

4 CONCLUSIONS

From the test results obtained in a series of loading test on a set of model nailed sand slopes using various types of facing, the following conclusions can be derived:

1) Ultimate bearing capacity and ductility of nailed slopes increases effectively by using rigid facing panels to which the head of nails are connected.
2) The use of panel facings with a local or global bending stiffness (facing types 2 and 3) effectively increase the tensile reinforcement force, in particular adjacent to the back of the facing.
3) Relatively high tensile reinforcement force including a high value in back of the facing measured in

Test No.3 are consistent with the highest value of footing pressure (i.e., the highest stability) in this test among all the tests investigated.

REFERENCES

Huang, C.C., Mikami, N., Okazaki, K. Hirakawa, D. and Tatsuoka, F. (2007) "Stability analysis of nailed sand slope with facing" Proc. 5th Int. Sympo. on Earth Reinforcement, IS Kyushu '07- New Horizon in Earth Reinforcement, Nov. 14–16, 2007 at Kyushu University, Fukuoka, Japan.

Huang, C.C., Tatsuoka, F. and Sato, Y. (1994) " Failure mechanisms of reinforced sand slopes loaded with a footing" Soils and Foundations, Vol. 34, No. 2, pp. 27–40.

Gutierrez, V. and Tatsuoka, F. (1988) "Role of facing in reinforcing cohesionless soil slopes by means of metal strips" Proc. Int. Geotech. Sympo. On Theory and Practice of Earth Reinforcement, Fukuoka, Japan. Yamanouchi, T., Miura, N. and Ochiai, H (Eds.), Balkema, pp. 553–558.